Optimal Parameterization of a Polarimetric DInSAR Model for SM Retrieval over Vegetated Agricultural Fields

Henri Schauer[1,2], Nikita Basargin[1,3,4], Simon Zwieback[5], Irena Hajnsek[1,2]

[1] German Aerospace Center, Oberpfaffenhofen, Germany;
[2] Institute of Environmental Engineering, ETH Zurich, Zurich, Switzerland
[3] School of Life Sciences, Technical University of Munich (TUM), Freising, Germany;
[4] Munich School for Data Science (MUDS), Munich, Germany;
[5] University of Alaska, Fairbanks, USA

Structure

1. Introduction
2. How Does Vegetation Impact the Interferometric Phase?
3. Bare Soil Models
4. Combined Model for Soil Moisture & Vertically Oriented Vegetation
5. Conclusion & Outlook

DInSAR Geometry enables phase-based soil moisture (SM) retrieval

DInSAR minimizes geometric effects by using a repeat-pass, zero-baseline configuration.

Deformation biases from SM changes of ~20% commonly exceeded 2 cm at HH

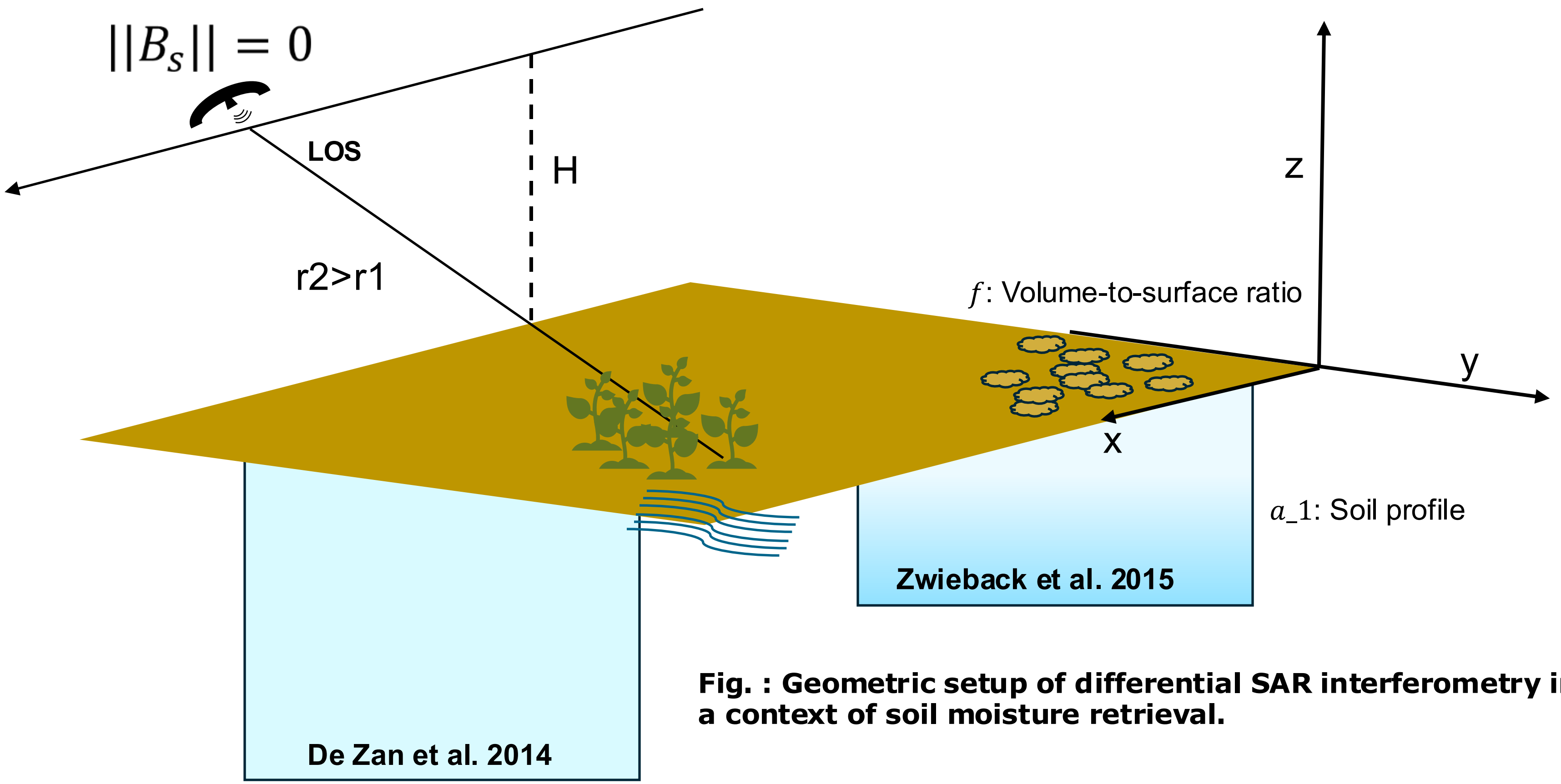

Fig. : Geometric setup of differential SAR interferometry in a context of soil moisture retrieval.

Data: AgriROSE-L Campaign

AgriROSE-L Airborne Campaign (F-SAR)

Terrabytes worth of data

- 23 flights over an agricultural region in Puch/Eitelsried, Bavaria.
- Full-polarimetric (HH, VV, HV, VH) at C-band & L-band (0.6 m × 1.29 m) .
- 3–6 days between acquisitions, allowing monitoring of growth season (e.g., April: surface scattering, July: volume scattering).
- **Key Observations:**
  - Evidence of seasonal scattering changes (Fig. 2)
  - Phenomenon of "flashing fields" (resonance effect) in many areas, though not the primary study focus.

Details about the Campaign:
Session: Future SAR missions and concepts 2
Time: 17.June: 11:10am-12:50am
Location: Aula Duza 2

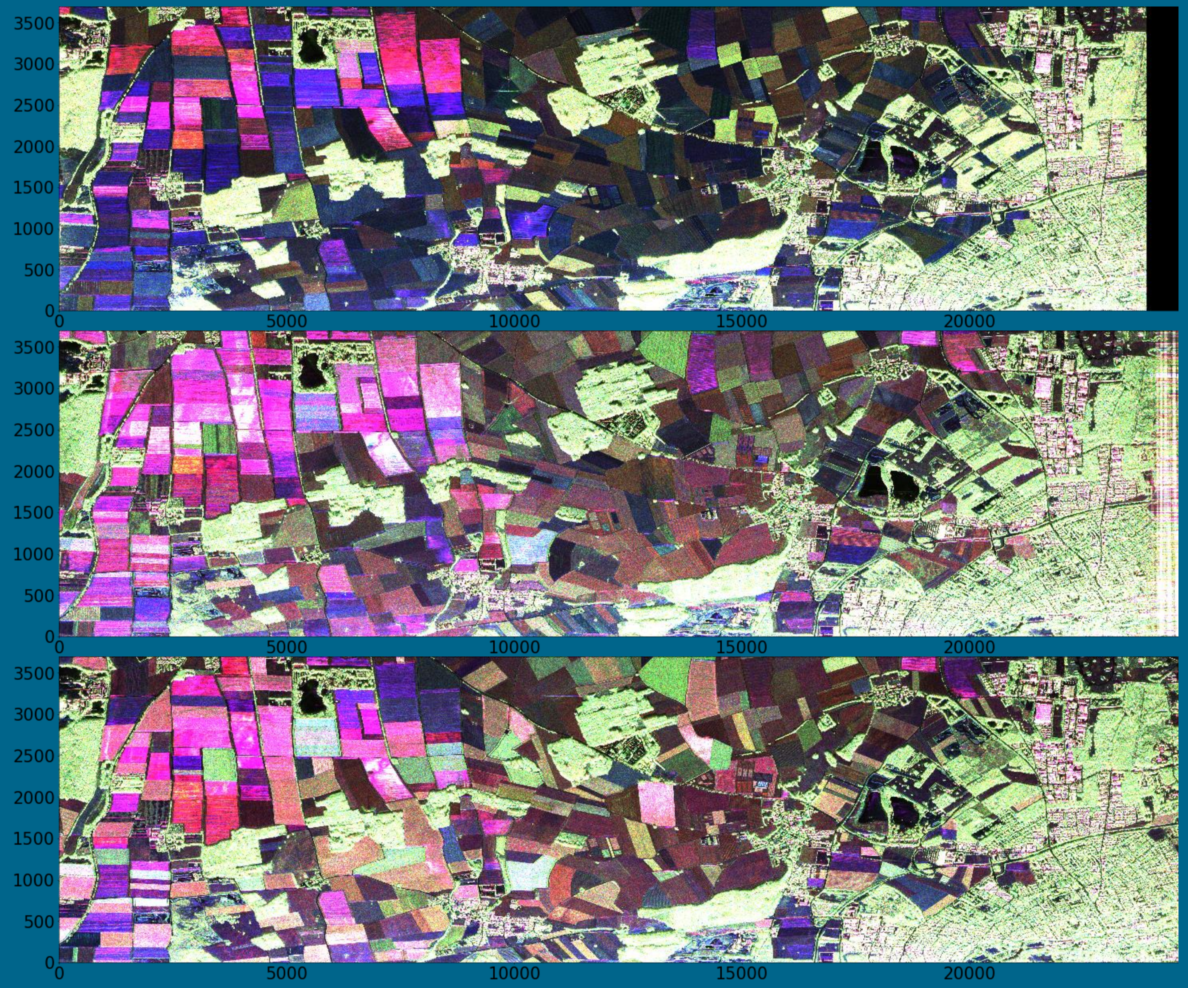

Fig. : Pauli RGB images from the F-SAR CROPEX 2025 campaign in L-band for the April 22nd (top), June 3rd (middle) and July 15th (bottom) with HH+VV, HH-VV, and HV+VH polarizations in blue, red, and green

Ground Truth

Fig. : Images of maize, maize, and potato fields for three dates. Bare soil conditions until the beginning of June for maize and potato.

- Dense SM measurements (every 50 m) using Delta-T Theta Probe MLX2 + HH2 logger across 3 crops (maize, potato, wheat)
- Additional field records: vegetation/soil roughness imagery + notes on dew, weather, and surface features
- Crop growth phases: wheat already 10 cm tall by April 22, maize planted ~May 16, potatoes ~one week later
- Additionally parameters covered by LMU at Puch site: plant type, dry biomass, plant geometry, leaf wetness, surface roughness
- No extensive vegetation data yet!
- In-situ data limitations: Heterogeneous soil conditions (roughness, type, clay content) not captured, potential Kriging interpolation errors; Depth integration mismatch between L-band and ground sensors

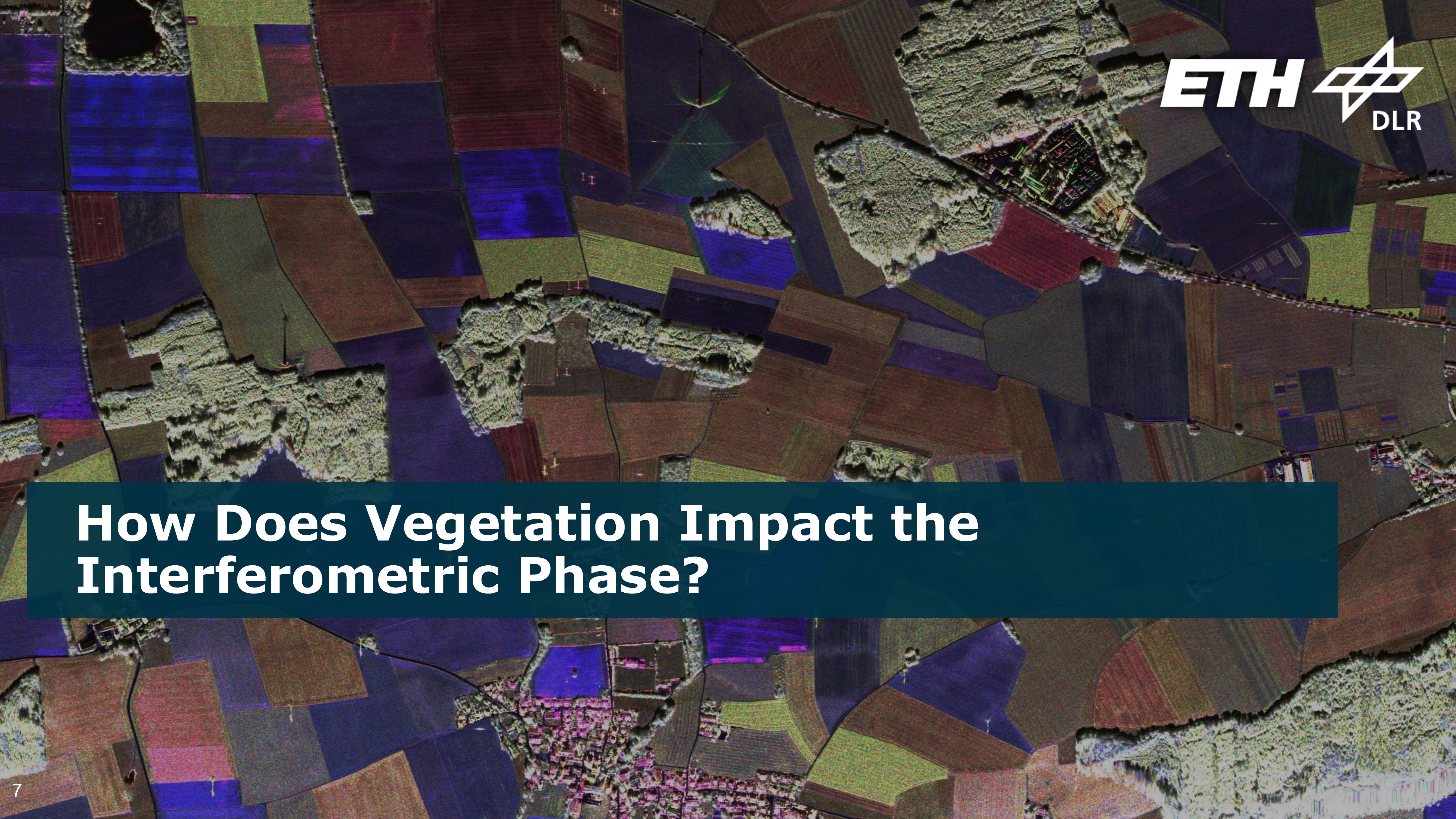

How Does Vegetation Impact the Interferometric Phase?

HH and VV Phase Differences – A Literature Review

Direct diagnostic of dieletric or structural changes of observed media

- Vegetation causes a phase shift that can be positive or negative, and importantly it's a per-polarization effect
- Phase similarity depends on medium anisotropy, polarimetric diversity in the scattering phase, dichroism, differential movement of dominant scatterers, noiselike decorrelation, multiple scattering (volume) (Zwieback et al., 2017)
- Bare soil: small polarimetric copolar phase differences (~10–20° at 6 days); Polarization-dependency of phase to soil moisture (Rabus et al., 2010; Zwieback et al., 2015)
- Vegetated soil: possibly large HH–VV difference (10–90°+ at 6 days) depending on vegetation structure and type
- In this study: displacement and ionospheric influence assumed negligible due to airborne data and the use of phase triplets

Mapping DInSAR over Vegetated Soils

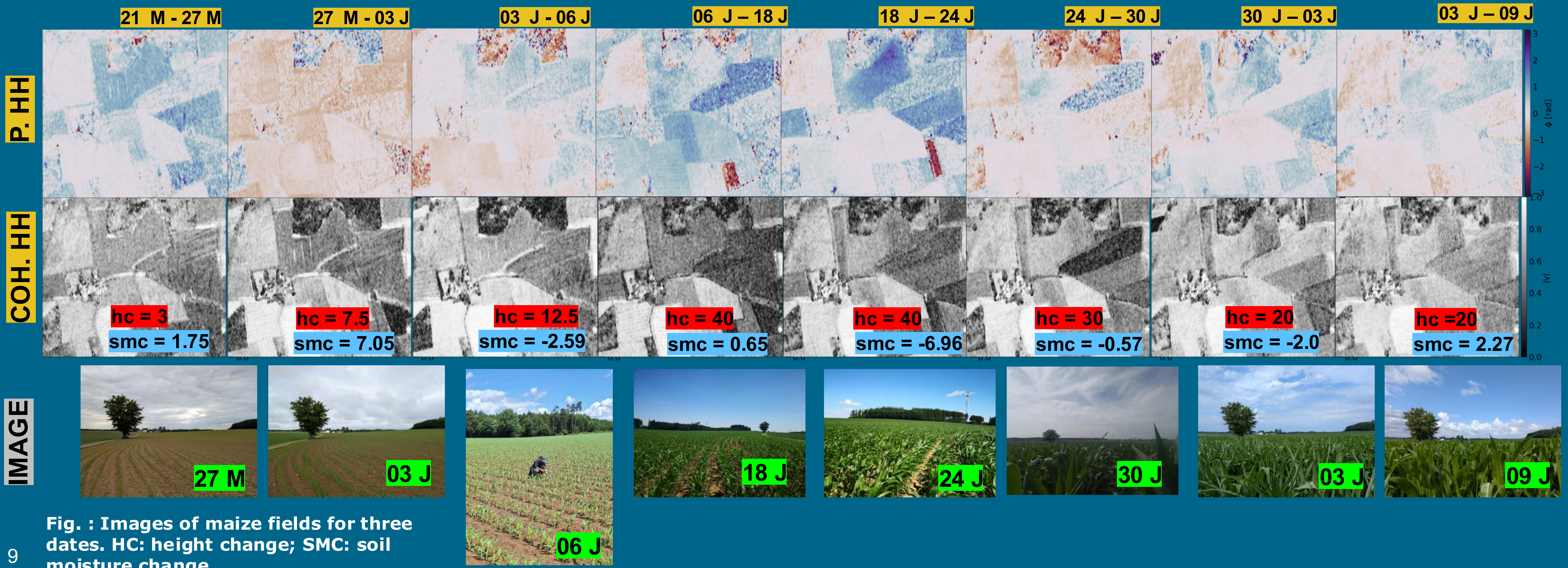

Fig. : Images of maize fields for three dates. HC: height change; SMC: soil moisture change.

DInSAR Polar Analysis Over Maize

18 J – 24 J

24 J – 30 J

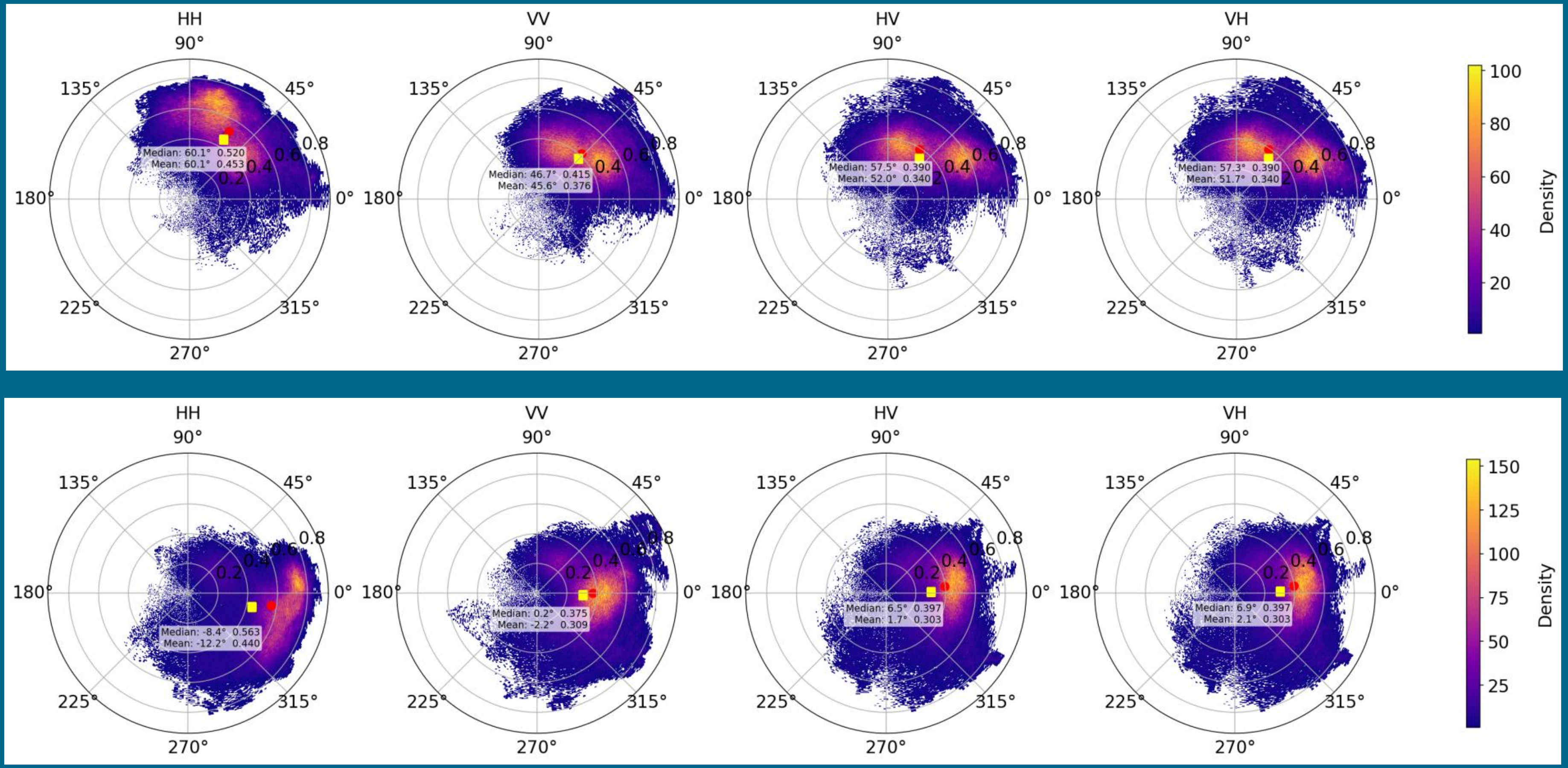

Fig. : Polar plots of observed HH vs. VV phase for increasingly vegetated soil condition over the maize field.

Inversion/ Adjustment Computation

Model Adjustment

We aim to statistically find the SM value that best predicts our reference F-SAR data.

- Time series optimization
- Optimize the other N-1 moisture values to minimize loss L

Mod. phase triplet — Obs. phase triplet — Mod. coherence — Obs. coherence

$$L = \sum_{(n>m>k)} \left| \varphi_{(n,m,k)} - \varphi'_{(n,m,k)} \right|^2 + \sum_{(n>k)} \left| \gamma_{(n,k)} - \gamma'_{(n,k)} \right|^2$$

Eq. : Loss function used for soil moisture inversion based on triplets and coherence.

- Adam optimizer with 180 iterations applied to multi-looked reference coherence and triplets (100 looks)
- Model inversion applied to all dates
- Validation done using the sampled three reference fields.

…

- Different learning rates for parameters
- Coherence < 0.35 masked out before inversion
- Realistic clamping for all geophyiscal variables and parameters
- Start values: sm=0.19, N=100, h=1, mv = 0.3

SM Estimation with Zwieback et al. (2015)

Estimates for Entire Dataset (a = -0.24, f = 0.3020, rms = 0.01, sand = 31.4 %, clay =20.4%))

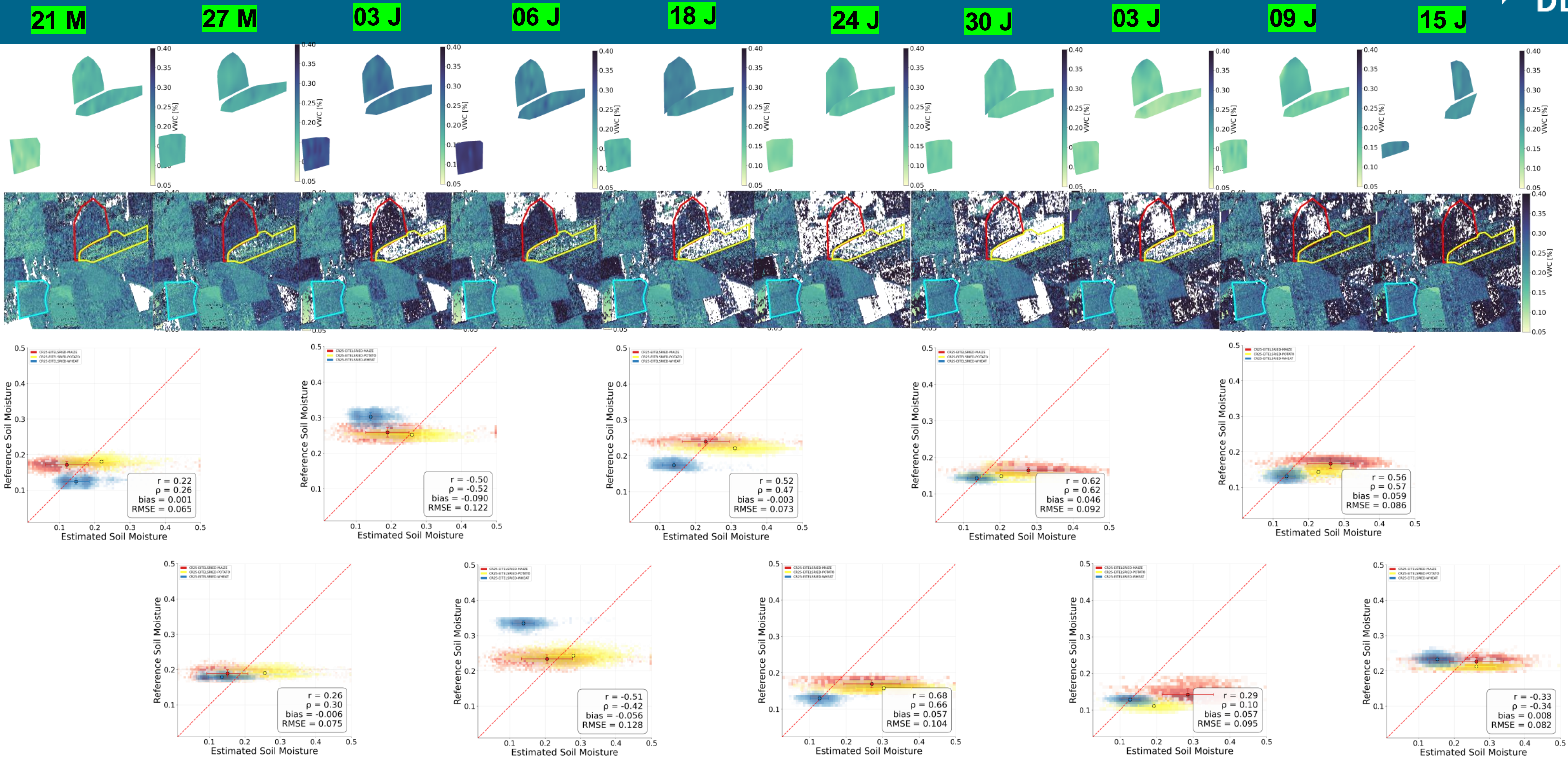

Fig. : Comparison between estimated and observed soil moisture as retrieved by the Zwieback standalone model. Scatterplots for each dates below.

SM Estimation using a Zwieback and Simple Vegetation Cylinder Combination

Model Combination

The total InSAR coherence is modelled as the product of soil and vegetation coherence, weighted by a mixing coefficient α.

$$\gamma_{total} = \gamma_{\mathrm{soil}} \cdot \left(\gamma_{veg}^{-\alpha}\right)$$

Eq. : Simple mixing of soil and vegetation model using weighting factor α.

- We partially compensate for both magnitude and phase using alpha
- E.g.: setting alpha = -0.5 will subtract 50% of the vegetation phase
- Only VV is modelled
- **Assumption**: no dihedral scattering, zero-baseline SAR data are not influenced by the height of the scatterers

- **Parameters:**
  1. Vegetation: Density, Stalk Dielectrics, Height = 1, r = 0.002
  2. Soil: Moisture, f, a1
  3. Additional: α

Cylinder Representations

Tab. : Electromagnetic cylinder representations according to Ruck et al. 1970.

	Low-Freq Infinite-Cylinder	Bessel/Mie
Radius Size (ka)	≪ 1	Any
Length Size (kL)	≫ 1	Infinite Cylinder Canonical
Dielectric Contrast (ε_r)	Any (ka ≪ 1)	Any, including wet/high-contrast
Mathematical Core	VV: $k^2a^2/4 \cdot (\varepsilon_v - 1)/\cos(\psi)$ HH: adds $2/(\varepsilon_v+1)$	Series $\Sigma\, a_n H_n^{(1)}$, boundary matched
Internal Field Assumption	Quasi-static internal field	Solved exactly
Computational Cost	Minimal (closed form)	Medium (~3–5 terms)

Problem: Thickening stalk or rising frequency

Sensitivity Analysis Electrically Thin Cylinder

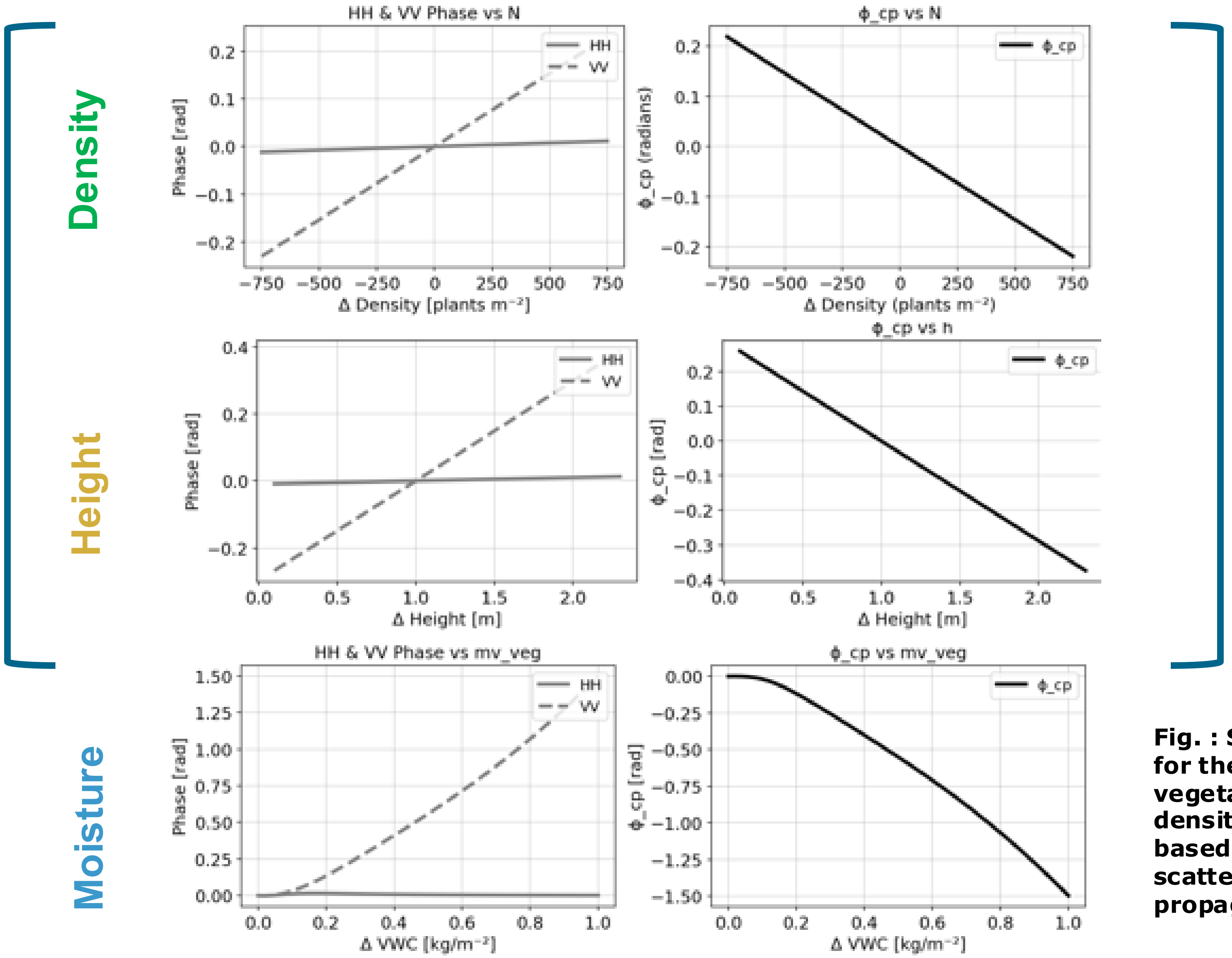

Fig. : Sensitivity analysis for the variables of the vegetation model (height, density, and moisture) based on the forward scattering matrix and the propagation phase.

Estimates for Entire Dataset using Combined Model (a1=-0.05, f=0.65, rms=0.01, r=0.02, alpha = -0.5)

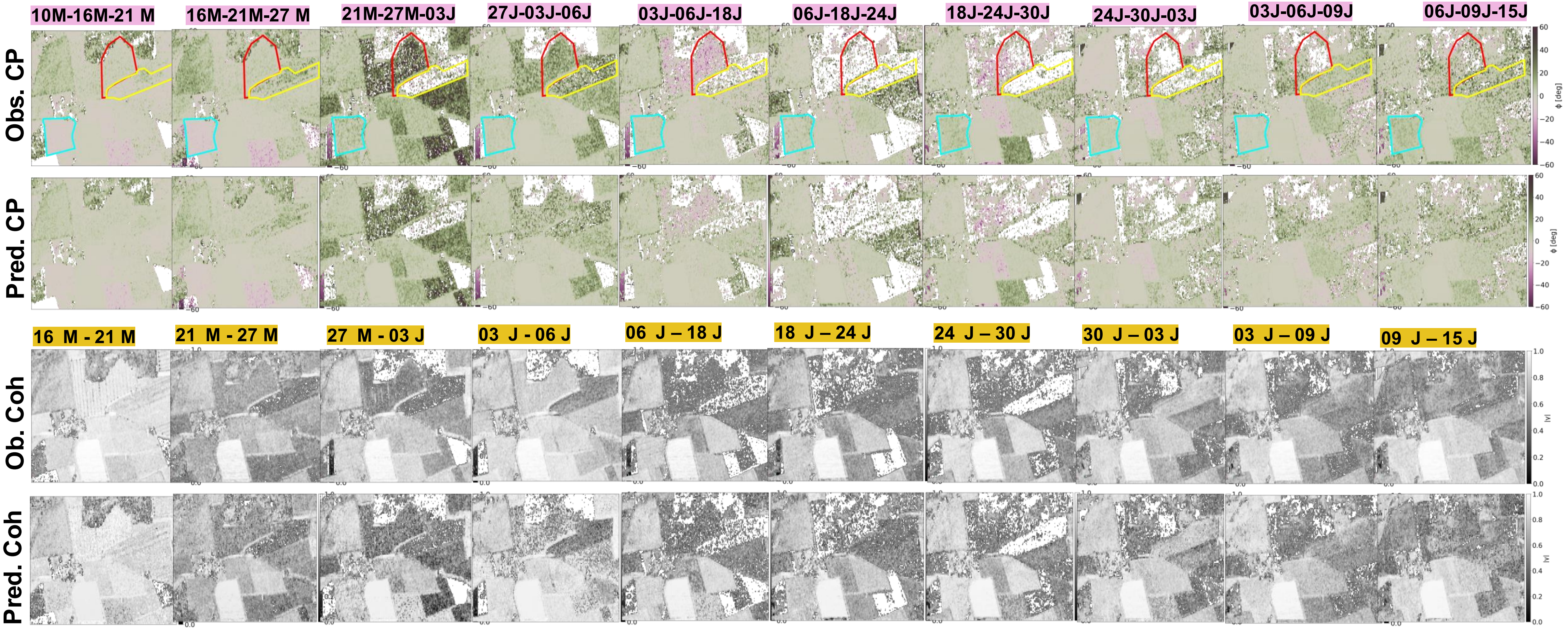

Fig. : Observed and predicted coherence and triplets from combined model in comparison for all dates starting from 21st of May.

Estimates for Entire Dataset (a1=-0.05, f=0.65, rms=0.01, r=0.002, alpha = -0.5)

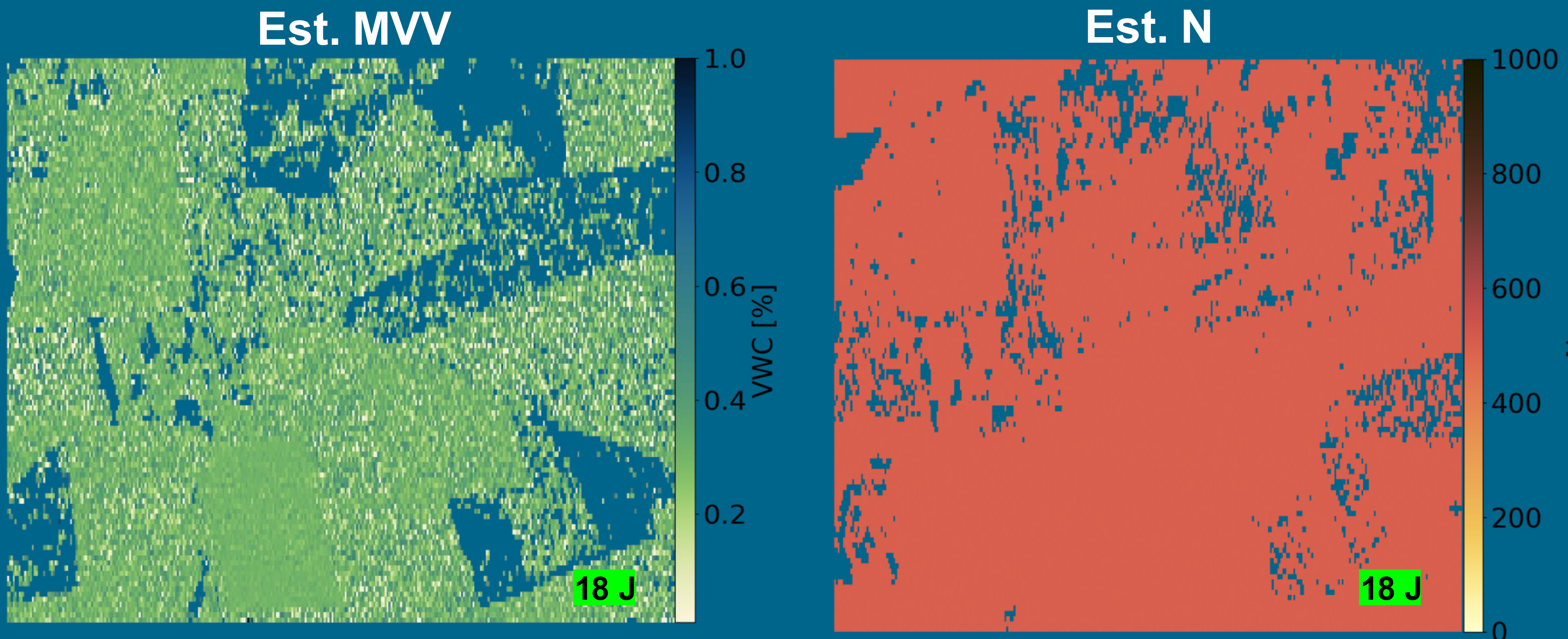

Fig. : Predicted vegetation variables retrieved for the entire time-series based on the combined model.

Estimates for Entire Dataset (a1=-0.05, f=0.65, rms=0.01, r=0.02, alpha = -0.5)

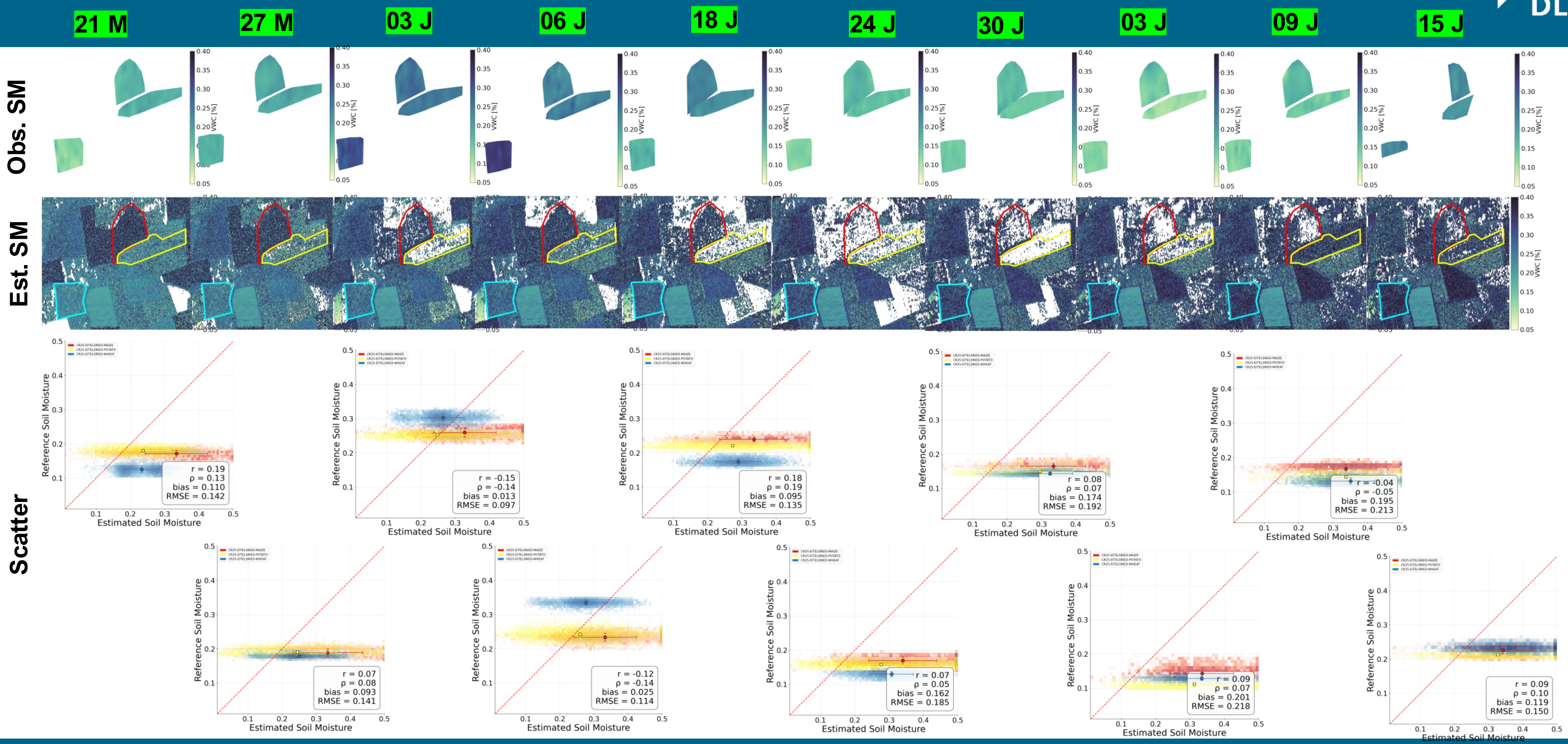

Fig. : Comparison between estimated and observed soil moisture as retrieved by the combined model. Scatterplots for each dates below.

Error Metrics Field maize

Tab.: Comparison of error metrics for different models and model combinations.

	De Zan (HH)	De Zan (VV)	De Zan (VV) Bare	De Zan (HH) Bare	Zwieback HH	Zwieback VV	Zwieback HH Bare	Zwieback VV Bare	Combined Zwieback Cyl. VV
Pearson	**0.26 ± 0.1**	**0.3 ± 0.15**	0.27 ± 0.17	0.22 ± 0.17	0.2 ± 0.15	0.18 ± 0.2	**0.29 ± 0.27**	**0.23 ± 0.4**	0.12 ± 0.18
RMSE	0.05 ± 0.01	0.05 ± 0.01	0.05 ± 0.02	**0.04 ± 0.02**	**0.04 ± 0.01**	**0.04 ± 0.01**	**0.04 ± 0.02**	0.05 ± 0.015	0.07 ± 0.01
Bias	-0.001 ± 0.03	0.003 ± 0.02	-0.006 ± 0.005	**-0.002 ± 0.007**	0.003 ± 0.02	0.01 ± 0.02	**-0.002 ± 0.02**	0.01 ± 0.02	-0.01 ± 0.04

Conlusion and Discussion

Vegetation estimation using the polarimetric interferometric phase is only partly solved

- Small HH-VV phase differences for SM
- HH-VV phase differences for vegetation depend on orientation and dielectrics
- Vertically-Oriented Vegetation can be successfully estimated with various cylinder approximations (low-frequency infinite cylinder approx. to full bessel cylinders)
- Depending on model-combination and parametric setup, SM estimation can be adapted to vegetation presence (vertically oriented)
- BUT: Forward model development, check ambiguities
- Use of dCPD inside model? Recover HH sensitivity with appropriate cylinder?
- Models effectively usable for large datasets questionable
- Estimation of randomly-oriented vegetation?

Interferometric phase is sensitive to SM change, however the models need to be adapted to account for adaptive roughness and vegetation

FRINGE 2026

Thanks for your attention!

Contact: henri.schauer@dlr.de

Krakow, Poland, 16 June 2026

ETH DLR

Mapping DInSAR over Vegetated Soils

Fig. : Images of maize fields for three dates. HC: height change; SMC: soil moisture change.

APA Reference List 1

De Zan, F., Parizzi, A., Prats, P., & López-Dekker, P. (2014). A SAR interferometric model for soil moisture. *IEEE Transactions on Geoscience and Remote Sensing*, *52*(1), 418–425. https://doi.org/10.1109/TGRS.2013.2241069

De Zan, F., Zonno, M., & López-Dekker, P. (2015). Phase inconsistencies and multiple scattering in SAR interferometry. *IEEE Transactions on Geoscience and Remote Sensing*, *53*(12), 6608–6616. https://doi.org/10.1109/TGRS.2015.2444431

Liu, G., Ding, X., Wu, S., Peng, W., Zhu, J., & Fu, H. (2025). Experimental study of L-band and S-band SAR signal penetration into soil and hard surface. *The International Archives of the Photogrammetry, Remote Sensing and Spatial Information Sciences*, *XLVIII-G-2025*, 967–972. https://doi.org/10.5194/isprs-archives-XLVIII-G-2025-967-2025

Liu, G., Fu, H., J. Zhu, Wang, C., & Xie, Q. (2021). Penetration depth inversion in hyperarid desert from L-band InSAR data based on a coherence scattering model. *IEEE Geoscience and Remote Sensing Letters*, *18*(11), 1981–1985. [https://doi.org/10.1109/LGRS.2020.3011706](https://www.google.com/search?q=https://doi.org/10.1109/LGRS.2020.3011706)

Luo, J., Lopez-Sanchez, J. M., & Hajnsek, I. (2025). Sensitivity analysis of co-polar complex coherence for crop monitoring at L-band. *IEEE Journal of Selected Topics in Applied Earth Observations and Remote Sensing*. [https://doi.org/10.1109/JSTARS.2025.3528144](https://www.google.com/search?q=https://doi.org/10.1109/JSTARS.2025.3528144)

Ruck, G. T., Barrick, D. E., Stuart, W. D., & Krichbaum, C. K. (1970). Radar cross section handbook. Plenum Press.

APA Reference List 2

Ulaby, F. T. (1980). Snowcover influence on backscattering from terrain. *IEEE Transactions on Antennas and Propagation*, *28*(6), 823–829. [https://doi.org/10.1109/TAP.1980.1142426](https://www.google.com/search?q=https://doi.org/10.1109/TAP.1980.1142426)

Ulaby, F. T., Held, D., Donson, M. C., McDonald, K. C., & Senior, T. B. A. (1987). Relating polarization phase difference of SAR signals to scene properties. *IEEE Transactions on Geoscience and Remote Sensing*, *GE-25*(1), 83–92. https://doi.org/10.1109/TGRS.1987.289787

Ulaby, F. T., Sarabandi, K., & McDonald, K. (1993). L-band SAR co-polarized phase difference modeling for maize fields. *IEEE Transactions on Geoscience and Remote Sensing*, *31*(1), 191–202. https://doi.org/10.1109/36.210459

Zwieback, S., Hensley, S., & Hajnsek, I. (2015a). Assessment of soil moisture effects on L-band radar interferometry. *Remote Sensing of Environment*, *164*, 77–89. https://doi.org/10.1016/j.rse.2015.04.012

Zwieback, S., Hensley, S., & Hajnsek, I. (2015b). A polarimetric first-order model of soil moisture effects on the DInSAR coherence. *Remote Sensing*, *7*(6), 7571–7596. https://doi.org/10.3390/rs70607571

Zwieback, S., & Hajnsek, I. (2016). Influence of vegetation growth on the polarimetric zero-baseline DInSAR phase diversity—Implications for deformation studies. IEEE Transactions on Geoscience and Remote Sensing, 54(5), 3070–3082. https://doi.org/10.1109/TGRS.2015.2511118

Zwieback, S., Hensley, S., & Hajnsek, I. (2017). Soil moisture estimation using differential radar interferometry: Toward separating soil moisture and displacements. *IEEE Transactions on Geoscience and Remote Sensing*, *55*(9), 5069–5083. [https://doi.org/10.1109/TGRS.2017.2704323](https://www.google.com/search?q=https://doi.org/10.1109/TGRS.2017.2704323)